Critical viscosity of the ionic mixture triethyl *n*-hexyl ammonium triethyl *n*-hexyl borate in diphenyl ether

Simone Wiegand,[a] Robert F. Berg,[b] and Johanna M. H. Levelt Sengers
Physical and Chemical Properties Division, National Institute of Standards and Technology, Gaithersburg, Maryland 20899

(Received 3 October 1997; accepted 15 June 1998)

We report measurements of the viscosity near the consolute point of triethyl *n*-hexyl ammonium triethyl *n*-hexyl borate in diphenyl ether. Until recently, this ionic mixture was the leading candidate for a ''mean-field'' ionic fluid composed of small molecules. The measurements of the coexistence curve of Singh and Pitzer and the measurements of turbidity of Zhang *et al.* had indicated mean-field static behavior. In contrast, the present measurements show a critical viscosity enhancement similar to that seen in Ising fluids. Such an enhancement is not expected in either a mean-field fluid or a fluid with sufficiently long-ranged forces. The measurements were made in two very different viscometers. Both viscometers achieved low shear rates by use of a flow impedance larger than in a conventional capillary viscometer. The first viscometer's impedance was a glass frit consisting of about 10^5 pores of 5.5 μm diam each. The second viscometer's impedance was a single 1 m long, 203 μm diam capillary. In both viscometers, the sample was sealed entirely in glass, in order to inhibit decomposition of the sample. © *1998 American Institute of Physics.* [S0021-9606(98)52235-0]

I. INTRODUCTION

Over the last decade, researchers have studied about a dozen different ionic mixtures near their critical consolute points in order to find a system having both long-range Coulombic interactions and a critical temperature sufficiently close to room temperature to allow accurate measurements. The motivation was the expectation that mixtures with long-range interactions might show departure from Ising-type critical behavior. Although it is recognized that Debye screening makes the Coulombic interactions effectively short-ranged, it is still an open question as to how the Debye screening length affects the critical fluctuations. Most well-known ionic solutions either have no convenient consolute temperature, or they have an Ising-type phase separation which is driven by nonelectrostatic forces. The most promising mixtures have been partly dissociated salts dissolved in nonaqueous fluids of low dielectric constant, in which Coulombic forces might dominate. A summary of the recently studied ionic mixtures can be found in a chapter by Levelt Sengers *et al.*[1,2] and in an article by Pitzer.[3] Almost all of these mixtures showed asymptotic Ising-type critical behavior.

Only one ionic mixture has shown mean-field behavior over a broad temperature range, namely the organic salt triethyl *n*-hexylammonium triethyl *n*-hexylborate ($N_{2226}B_{2226}$) dissolved in diphenyl ether. The first indication of mean-field behavior was found by Singh and Pitzer,[4,5] who measured the coexistence curve. In the region $\epsilon > 10^{-3}$, a log–log plot of their data showed a slope of 0.476,[1] consistent with the mean-field exponent $\beta = \frac{1}{2}$. In the region $\epsilon < 10^{-4}$, the data could be fit with either a mean field or an Ising-type expression. Here $\epsilon = (T - T_c)/T_c$ is the reduced temperature and T_c is the critical temperature. A second indication of mean-field behavior was found by Zhang *et al.*,[6] who measured turbidity in the range of reduced temperatures $10^{-4} < \epsilon < 10^{-1}$. They found $\gamma = 1.01 \pm 0.01$, where γ is the critical exponent for the susceptibility. The mean-field value for γ is one. However, the turbidity measurements were repeated recently for a mixture prepared from the same, newly synthesized, sample of salt used here. The new turbidity measurements did not confirm the earlier data.[7]

Here we report measurements of the viscosity near the consolute point of $N_{2226}B_{2226}$ in diphenyl ether. In contrast to the previous indications of mean-field static behavior, our results are consistent with the viscosity anomaly shown by fluids in the Ising universality class.

A. Viscosity as a measure of non-Ising behavior

Near the critical point of an Ising fluid, the viscosity η is characterized by an exponent y according to[8–10]

$$\eta = \eta_B (Q_0 \xi)^{x_\eta} = \eta_B (Q_0 \xi_0)^{x_\eta} \epsilon^{-y}. \tag{1}$$

The noncritical or background viscosity is η_B, and the divergence amplitude $(Q_0 \xi_0)^{x_\eta}$ contains the product of the fluid-dependent wave vector Q_0 and the correlation length amplitude ξ_0. Q_0 is a system-dependent critical amplitude related to a microscopic cutoff parameter in mode-coupling theory.[11] The viscosity exponent

$$y = x_\eta \nu, \tag{2}$$

is the product of ν, the critical exponent of the correlation length, and the exponent x_η. Hao and co-workers[12] recently performed a two-loop mode-coupling calculation of x_η of an Ising fluid. Their result was $x_\eta = 0.066$ ($y = 0.042$). This

[a]Present address: Institut für Anorganische und Physikalische Chemie, Universität Bremen, Leobener Strasse, 28334 Bremen, Germany.
[b]E-mail: robert.berg@nist.gov

value agrees with the range measured in conventional mixtures. For example, Berg and Moldover[13] measured $0.0404 < y < 0.0444$ for four binary fluid mixtures.

Because the viscosity exponent y is sensitive to the coupling between velocity and concentration fluctuations, it is a measure of the fluid's Ising character. The theory for the viscosity divergence near the critical point of a fluid with long-range interactions is not well established. Nevertheless, there are two theoretical views which predict that the divergence, if any, should be weaker than that of an Ising fluid. In the framework of the renormalization group theory, Folk and Moser[14] found that the exponent x_η depends on the range of the intermolecular forces. Their results were stated in terms of the exponent σ which parameterizes forces which decay with distance r according to $r^{-3-\sigma}$. The value of x_η varied smoothly from zero at $\sigma=1$ to the value associated with short-range forces at $\sigma=2$. No divergence was expected for $\sigma<1$. In the framework of the mode–mode coupling theory, Douglas[15] argued that the exponent x_η would be zero in a mean-field fluid due to the absence of coupling between the velocity and concentration fluctuations. Finally, we mention that an early calculation by Mountain and Zwanzig[16] based on hard spheres interacting through a long-range potential found no anomaly in the viscosity.

The absence of a viscosity anomaly in a mean-field fluid would differ qualitatively from the value $y=0.04$ in an Ising fluid. Another critical exponent which might be expected to have such a qualitative difference is the heat capacity exponent α. Jacobs and co-workers,[17] however, argue that, in the present mixture, the heat capacity anomaly would be too small to allow distinguishing $\alpha=0$ from the Ising value $\alpha=0.11$. For Ising systems, two-scale factor universality gives a relation[18,19] between the amplitude of the heat capacity A^+ and the amplitude of the correlation length ξ_0

$$A^+=\frac{k_B X}{\xi_0^3}. \tag{3}$$

Here k_B is Boltzmann's constant, and $X\simeq 0.019$ is a universal ratio.[20] The value of ξ_0, which lies between 1 and 1.4 nm for $N_{2226}B_{2226}$,[7] is an order of magnitude larger than that typical of binary mixtures of small molecules. This implies that the heat-capacity anomaly would be very small, at least 700 times smaller than observed in triethylamine-water, for example. Viscosity is thus superior to heat capacity for distinguishing Ising from mean-field behavior.

B. Previous viscosity measurements

Only two measurements of the viscosity near the critical point of a nonaqueous ionic mixture have been reported. For tetra-*n*-butylammonium picrate in tridecanol, Kleemeier *et al.*[21] found a critical anomaly with the viscosity exponent $y=0.043\pm 0.001$, where the uncertainty was due to the uncertainty in the measured value of T_c. This result is consistent with the viscosity exponents found in nonionic Ising-type systems,[13,22] even though turbidity measurements[23] had found mean-field behavior in a limited range of temperature.

For ethylammonium nitrate in *n*-octanol, Oleinikova and Bonetti[24] found that the viscosity exponent depended on the choice of background and crossover function fitted to their data, with y falling in the range $0.0289\leqslant y\leqslant 0.0324$. When they allowed T_c to be a free parameter, the range became $0.0385\leqslant y\leqslant 0.0438$. Thus the viscosity of this system is apparently Ising-type. This is to be expected, because light scattering measurements[25] also yielded Ising exponents.

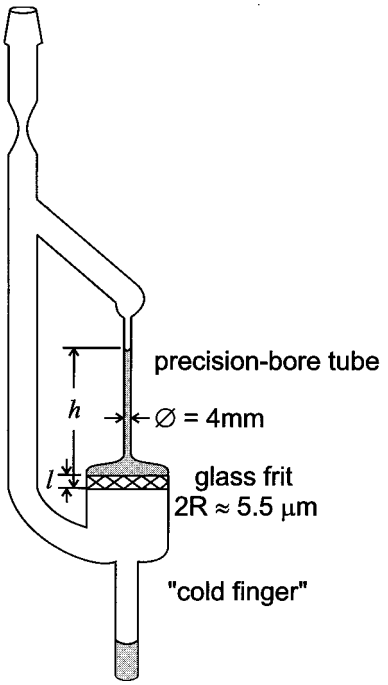

FIG. 1. Sketch of the frit viscometer. As the sample drained through the frit, the height h of the liquid contained in the precision-bore tube fell with an exponential time dependence.

C. Two viscometers

The measurements reported here were made in two very different viscometers. Each viscometer was of a novel design which allowed a shear rate much lower than in a conventional capillary viscometer. Shear thinning is an important consideration near the consolute points of ordinary mixtures. It is even more important for the recently studied nonaqueous ionic solutions, where typically both the salt and the solvent molecules may contain a dozen or more carbon atoms. Such systems are more sensitive to shear rate because the larger molecular size tends to increase both the viscosity and the correlation length amplitude.

In both viscometers, the sample was sealed entirely in glass, in order to inhibit decomposition of the sample. Both viscometers achieved low shear rates by use of a flow impedance larger than in a conventional capillary viscometer. The ''frit'' viscometer's impedance (Fig. 1) was a glass frit consisting of about 10^5 pores of 5.5 μm diam each. The ''spiral'' viscometer's impedance (Fig. 2) was a single 1 m long, 203 μm diam capillary. Glass viscometers with small capillaries have been used previously. For example, that used by Beysens *et al.*[26] had a diameter of 200 μm. However, our spiral viscometer's capillary was almost 10 times longer, but the pressure head was several times lower. Both viscometers

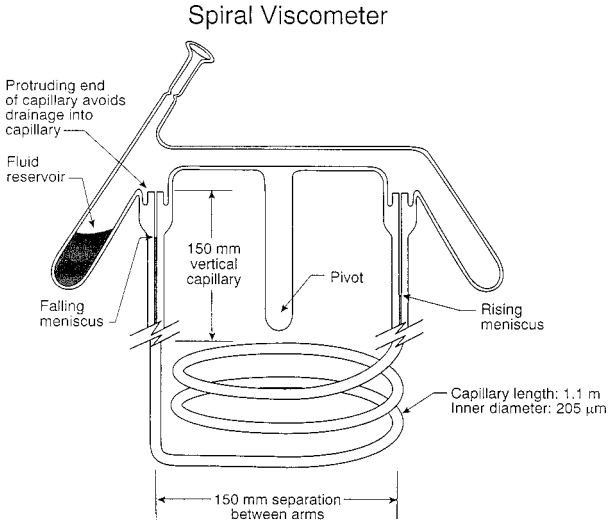

FIG. 2. Sketch of the spiral viscometer. A measurement was begun by temporarily tilting the viscometer to decrease the meniscus height in the right vertical capillary, then re-leveling the viscometer. The viscosity of the fluid contained in the capillary was inferred from the exponential return of the meniscus to its equilibrium position.

detected the divergence of the viscosity of the mixture; however, adsorption effects reduced the accuracy of the frit viscometer.

In the following, Secs. II and III deal with issues which are common to both viscometers, Sec. IV describes the frit viscometer and its results, and Sec. V does the same for the spiral viscometer.

II. VISCOMETER DESIGN CONSIDERATIONS

To measure accurately the viscosity of any fluid one must consider the sensitivity of the fluid to impurities and to shear rate. $N_{2226}B_{2226}$ in diphenyl ether is especially sensitive to both influences. Moreover, the small capillaries used in our frit viscometer required corrections for preferential adsorption. In what follows, we discuss the implications of these three effects for the design of the two viscometers.

A. Purity

At room temperature, the salt $N_{2226}B_{2226}$ is a colorless, highly viscous liquid which turns brown in the presence of oxygen or water. The sample deteriorates unless it is stored in an all-glass container. After two years of storage in a glass bottle with a rubber seal, the salt prepared for Zhang *et al.* had turned from colorless to brown–red and the critical concentration of the resulting solutions had shifted greatly. Ford and co-workers[27] also reported that the salt reacts with a rubber septum. Adding to the difficulty, this deterioration process is self-catalytic.[28] Singh[29] noticed that water lowers T_c while organic impurities increase T_c. Even samples prepared under nominally identical conditions can have widely varying critical temperatures. For example, Singh and Pitzer,[4,5] reported stable, reproducible phase separation temperatures within 1 K of 44 °C, more than 20 K higher than the critical temperature published by Zhang *et al.*[6] The critical temperatures of the three samples prepared by Zhang[30] varied from 16 °C to 23 °C, while those for the present samples varied between 36 °C and 39.5 °C.

B. Shear rate

In conventional viscometers, viscosity data close to the critical point are influenced by shear because the relaxation time Γ^{-1} of the critical concentration fluctuations diverges strongly (''critical slowing down'').[8] An influence of shear is expected when the rate of shear S is comparable to Γ or larger. Therefore, for a capillary viscometer, avoidance of strong shear-thinning requires the condition

$$S \leqslant \Gamma$$

or

$$\frac{4}{15}\frac{\rho g R h}{\eta l} \leqslant \frac{k_B T}{6\pi\xi_0^3\eta_B}\epsilon^{3\nu+y}. \tag{4}$$

Here R is the radius of the capillary, h is the height of the meniscus above the outlet of the capillary, l is the length of the capillary, g is the gravitational constant, and ρ is the density of the mixture. The strong dependence of this expression on the correlation length amplitude ξ_0, combined with the large value of ξ_0 for $N_{2226}B_{2226}$ in diphenyl ether, requires extremely low shear rates which cannot be obtained in a conventional capillary viscometer. For example, if one wants to measure at a reduced temperature of 10^{-4} with a typical ratio of $h/l \approx 1$, one needs a capillary with $R = 3\ \mu$m. Even if the sample volume is only that of the capillary, one viscosity measurement would last ~ 80 years.

In our two viscometers, the conflict between low shear rate and reasonable measurement time was resolved in different ways. The frit viscometer achieved a reasonable measurement time because it had the equivalent of 10^5 parallel capillaries, each of a small radius. The spiral viscometer did the same by use of a single, much larger capillary. Nevertheless its shear rate was low, because the combination of an unusually long capillary and a very small meniscus height difference resulted in $h/l \approx 0.01$.

C. Adsorption corrections

One of the mixture's components will be preferentially adsorbed onto the wall of the viscometer. The resulting change in composition affects the viscosity near the wall (see Fig. 3). Because this effect is important in a layer of thickness comparable to ξ, it was important in the frit viscometer, which had 5.5 μm diam pores. It was not important in the spiral viscometer, which had a 203 μm diam capillary.

To estimate the effect of adsorption, we have assumed that near the wall a layer forms in which the composition, and therefore, the viscosity, differs from the bulk value. We have assumed that the thickness of such a layer is proportional to the correlation length, which is consistent with the scaling theory of Fisher and de Gennes[31] in the strong-field limit. The viscosity shift has no explicit temperature dependence, but only a dependence on the thickness of the layer which scales as the correlation length.

III. PREPARATION OF $N_{2226}B_{2226}$ IN DIPHENYL ETHER

The $N_{2226}B_{2226}$ salt was custom-synthesized by StremChem,[32] a company specialized in metal-organic chemistry. Nuclear magnetic resonance (NMR) spectroscopy tests performed by the manufacturer confirmed that the composition was consistent with the chemical structure and that excess reactants had been removed. Boron NMR spectra indicated that the boron was not oxidized. The salt was shipped in glass bottles sealed under argon pressure by Teflon without a rubber septum. It had a very light pale yellow color, which had also been reported by Singh and Pitzer.[4,5] Its melting point, which we determined in a sealed glass ampoule, was $-24.5\,^{\circ}\mathrm{C}$. This is somewhat below the melting points found in the literature, which vary from $-21.6\,^{\circ}\mathrm{C}$ to $-22.5\,^{\circ}\mathrm{C}$.[4,6]

Diphenyl ether was purchased from Aldrich Chemical Company as a gold-label-grade chemical (higher-than-average purity). The diphenyl ether was degassed by repeated freezing and pumping in order to remove dissolved air.

We carefully avoided exposure of the sample to air and to moisture. The salt was handled exclusively in a glove box which was flushed with 99.9995% dry argon and maintained at a slight overpressure. All containers which were used during the sample preparation process were soaked in nitric acid at 50–70 °C for 4–6 h, repeatedly flushed with filtered, distilled, deionized water, and baked in air at 500 °C overnight. We did not observe any discoloration during the sample preparation, which lasted four days after the bottle was opened.

We first sealed several test samples with different concentrations and measured the phase volumes within 5 mK from the critical temperature. A fit to these data gave the critical concentration $x_c = 0.049 \pm 0.001$ in mole fraction of salt, where the uncertainty is one standard uncertainty from the fit. We then determined the density at the critical concentration with a 10 ml pycnometer which had been calibrated with water. The temperature dependence was $\rho/\rho^+ = 1.0665 - 8.366 \cdot 10^{-4} \times (T - T_0)$, where $\rho^+ = 1\ \mathrm{kg \cdot m^{-3}}$, $T_0 = 273.15$ K, and T is the temperature in Kelvin.

To prepare a batch at the critical composition we filled a flask with the estimated amount of salt and then added diphenyl ether until the desired mass fraction was achieved. The diphenyl ether was added last because its larger mass eased the final adjustment to the critical concentration. We then heated the inside of the glove box above the phase separation temperature and mixed the components. The homogenous mixture was transferred by syringe into the viscometers inside the glove box.

IV. FRIT VISCOMETER

A. Description

This viscometer incorporated a glass frit, produced commercially as a filter, which consisted of glass particles sintered to create a disk containing pores whose average diameter was 5.5 μm. The frit was fused into the 27 cm long glass assembly shown in Fig. 1. Above the frit was a precision-bore tube with an inner diameter of 4 mm. Below the frit was a collection reservoir and a cold finger. There were two reasons for the cold finger. First, in order to remove air from the mixture during the filling process, we repeatedly evacuated the viscometer after freezing the mixture. By immersing only the cold finger in liquid N_2 or in a mixture of ethanol and liquid N_2, we avoided thermal stresses which would crack the frit. Second, when the viscometer was immersed in the water bath just below T_c, we could check the criticality of the mixture. This was accomplished by placing all of the sample in the cold finger and then comparing the volumes of the two phases.

The frit's multiple capillaries had the advantage that it was insensitive to clogging of some of the fine capillaries. It had the disadvantage that it required a significant correction for preferential adsorption.

B. Cleaning and filling

The large flow impedance required to get low shear rates made the two viscometers difficult to clean. We developed a procedure which cleaned the frit viscometer thoroughly without changing the average diameter of the frit capillaries. We soaked the viscometer in nitric acid for 4–8 h at 70 °C. Then we rinsed the viscometer, first with distilled water, and then with water processed by a Milli-Ro10 Plus and Milli-Q UV-Plus with a 0.2 μm Teflon filter. The frit viscometer was dried in air at 500 °C overnight to remove moisture.

By filling the viscometer in the same glove box used for sample preparation, the salt never came in contact with air or water. Prior to the filling, the viscometer was kept in the glove box for one week. After the filling, it was connected to a glass Teflon valve by a connector sealed with a grease-free O-ring. It was then transferred out of the glove box and connected to the pumping system by an ultra-Torr vacuum connector. After freezing the sample in a mixture of ethanol and liquid nitrogen at a temperature below $-50\,^{\circ}\mathrm{C}$, we pumped on the viscometer. We repeated the freeze and pump process three times. Careful degassing was required to avoid bubbles in the frit's interior, which could cause errors in the measurements.

C. Operation

The viscometer was placed in a doubly insulated, vigorously stirred water bath whose temperature was controlled by a Tronac PTC-40 precision temperature controller. The overnight temperature stability was better than 5 mK. The temperature was measured by a platinum resistance thermometer which had been calibrated in the range from $-50\,^{\circ}\mathrm{C}$ to 250 °C with an uncertainty of less than 10 mK. The viscometer was mounted on a holder which had an external crank for rotation of the viscometer.

To determine T_c, we lowered the bath temperature by a small step, waited for 15–30 min, then gently shook the sample contained in the cold finger. Phase separation was indicated by transient inhomogeneities in the refractive index (Schlieren).

Before starting the measurements, we flushed the frit several times with the mixture. We then filled the precision capillary and the region just above the frit with the thor-

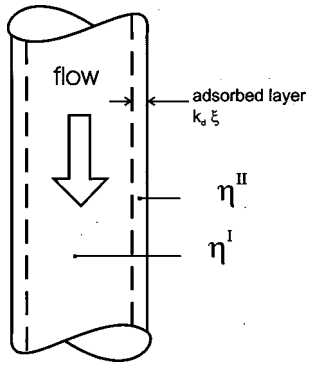

FIG. 3. Illustration of the adsorption correction model which was used for the frit viscometer. We assumed the existence of an adsorption layer composed entirely of the preferred phase. The layer's thickness $k_d\xi$ was assumed to be proportional to the correlation length.

oughly mixed sample. Often we had to shake the viscometer to remove all bubbles just above the frit. The position of the meniscus was measured by viewing it through a cathetometer while diffusely illuminating the precision capillary from the back. As the mixture drained through the frit, we recorded the position of the meniscus in the precision capillary as a function of time.

We made viscosity measurements at 20 temperatures, starting well above the phase separation temperature and then approaching T_c. Approximately 3–5 measurements were made at each temperature.

D. Model of the viscometer

1. Capillary array model

We modeled the flow in the frit viscometer as Poiseuille flow through an array of identical, parallel, cylindrical capillaries. For a single capillary[33] the velocity profile $u(r)$ is given by

$$u(r)=\frac{\Delta p}{4l\eta}(r^2-R^2), \tag{5}$$

where l and R are the length and radius of the capillary and Δp is the difference in pressure at the two ends. The volume flow through the entire array is given by

$$\dot{V}=A\dot{h}=-\frac{\pi\rho g R^4(h-h_0)}{8\eta l}N, \tag{6}$$

where h is the height of the meniscus in the precision-bore tube, A is the cross-section area of the precision capillary, ρ is the density, and N is the effective number of capillaries. Solving Eq. (6) with the boundary condition $h(0)=h_1$, the meniscus height thus falls exponentially in time

$$h(t)=h_0+(h_1-h_0)\exp\left(-\frac{\pi g R^4 N}{8lA}\frac{\rho}{\eta}t\right)$$
$$\equiv h_0+(h_1-h_0)\exp(-t/\tau), \tag{7}$$

where the constants h_0 and h_1 are obtained by fitting to the measurements of $h(t)$. The viscosity

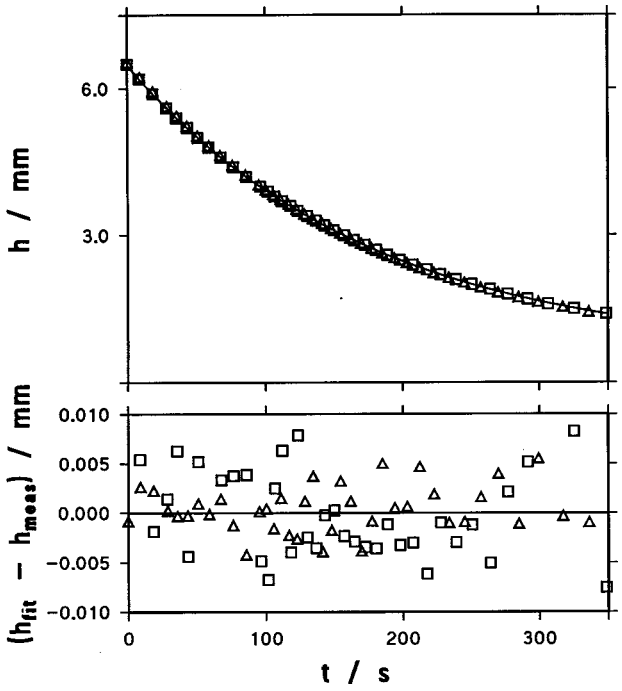

FIG. 4. Typical data set for the calibration of toluene in the frit viscometer. The time dependence of the height of the liquid meniscus could be described by a single exponential decay.

$$\eta=f_{\text{frit}}\tau\rho, \tag{8}$$

with $f_{\text{frit}}=(\pi g R^4 N)/(8lA)$, is directly proportional to the time constant τ in the exponential of Eq. (7). The viscometer's calibration constant f_{frit} is obtained by measurement with a fluid of known viscosity.

Appendices A, B, and C describe the corrections for adsorption, shear rate, and electrokinetic effects, respectively.

E. Calibration

We calibrated the frit viscometer with toluene. A typical data set for a calibration measurement at $T=20.5\ ^\circ\text{C}$ is shown in Fig. 4.

Similar measurements made with distilled, dust-free, deionized water disagreed with the toluene calibration constant by 1.6%. The explanation for this small discrepancy is possibly the differing surface tensions of water and toluene. The sample's surface tension and the curvature of the liquid meniscus at the viscometer's outlet created an interface pressure which added to the pressure difference Δp driving the fluid flow. This effect was studied in Ubbelodhe viscometers by Sengers *et al.*[34] They were unable to devise a model of this effect based solely on the surface tension and the geometry of the viscometer's outlet. Although our frit viscometer's geometry was such that it too was sensitive to surface tension, we did not include a correction for this effect. Because the surface tensions of the mixtures studied here are much less than that of water, we estimate that any correction for surface tension would be less than the 1.6% disagreement between the water and toluene measurements.

F. Fitting to the apparent viscosity

We derived the critical parameters $(Q_0\xi_0)^{x_\eta}$ and y of Eq. (1) by fitting to the viscosity data in the following manner. First, the viscometer's calibration constant was used to convert the measured exponential time constants τ into apparent viscosities η. Then, the apparent viscosity values were fit by

$$\eta = \eta^I \left\{ 1 + \left[\frac{\eta^I - \eta^{II}}{\eta^{II}} \right] \left[-4\left(\frac{k_d\xi}{R}\right) + 6\left(\frac{k_d\xi}{R}\right)^2 \right] \right\}, \tag{9}$$

where the ''bulk'' viscosity η^I was described by Eq. (B1),

$$\eta^I = \eta_B[1-\Delta(\lambda)](Q_0\xi_0)^{y/\nu}\epsilon^{-y}, \tag{10}$$

and the viscosity η^{II} in the wall layer of thickness $k_d\xi$ was defined to be that of the preferentially adsorbed component. The background viscosity η_B was determined from a noncritical sample (see Sec. IV G 2). The three fitted parameters were the dimensionless quantities $(Q_0\xi_0)^{y/\nu}$, y, and k_d.

G. Results

1. 2-butoxyethanol+water

We measured the viscosity of a critical mixture of 2-butoxyethanol+water to establish the performance of the frit viscometer on a well-known nonionic critical mixture. The 2-butoxyethanol had a purity of 99+% (Aldrich) and was used without further purification. The water was deionized, distilled, and filtered through a 0.2 μm filter. The critical composition at the lower critical point was determined by the criterion of equal volumes of coexisting liquid phases at 5 mK above T_c. We determined the critical mass fraction $y_c = 0.2945 \pm 0.0005$ from the condition of equal phase volumes within 5 mK from the critical point. The critical temperature, $T_c = (323.065 \pm 0.010)$ K, was within 3 K of previous measurements.[13,35–38] The uncertainty in T_c reflects the uncertainty stated by the manufacturer for the thermometer calibration. The bath's stability limited the reproducibility of T_c to 5 mK. After filling the viscometer with the critical mixture we degassed the sample by freezing and pumping three times as described previously.

During our preliminary measurements, which were made without the extensive cleaning procedure described earlier, the critical temperature changed by 2.5 K/week. This severe problem was attributed to impurities adsorbed onto the frit's large surface area. In particular, a trace of acetone increased the critical temperature and drastically shifted the critical concentration. During our final measurements, which benefited from a fresh sample and the improved cleaning procedure, the critical temperature drifted by less than 2 mK/week.

Figure 5 compares our results to those obtained by Berg and Moldover[13] and by Zielesny *et al.*[35] While the results agree with the previous measurements far from the critical temperature, the critical enhancement of the apparent viscosity is weaker. This difference was caused by preferential adsorption of water from the mixture onto the surface of the glass frit.

To fit to these data (Table I), we used the description of the density of Zielesny *et al.* at the critical concentration,[35] which is

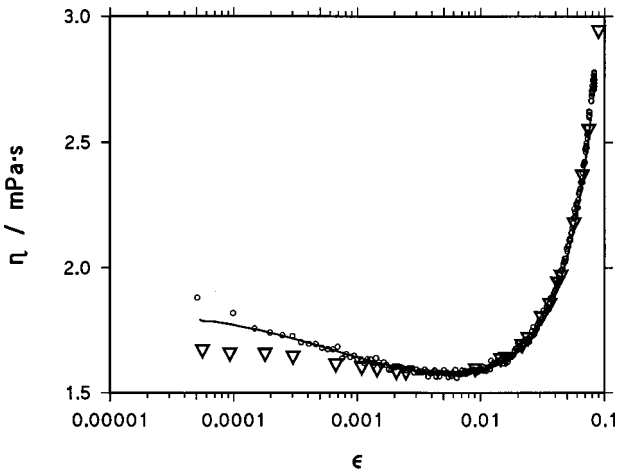

FIG. 5. Viscosity of the critical mixture of 2-butoxyethanol+water as a function of the reduced critical temperature ϵ. The curve represents the measurements by Zielesny *et al.* (Ref. 35), the open circles (○) are from Berg and Moldover (Ref. 13), and the open triangles (▽) refer to the present measurements in the frit viscometer. The data from Berg and Moldover have been divided by a factor of 1.045.

$$\rho/\rho^+ = a + b(T-T_0) + c(T-T_0)^2 + d(T-T_0)^3, \tag{11}$$

where $a = 0.991\,49$, $b = -5.544\times10^{-4}$ K^{-1}, $c = 3.208\times10^{-6}$ K^{-2}, $d = -1.883\times10^{-8}$ K^{-3}, $\rho^+ = 1$ kg·m^{-3}, $T_0 = 273.15$ K, and T is the temperature in Kelvin. (Their data were insufficiently accurate to see the expected weak critical anomaly). We also used their description of the background viscosity[35]

$$\eta_B = A \exp[B/(T-C)], \tag{12}$$

TABLE I. Shear viscosity η of the critical 2-butoxyethanol/water mixture measured in the frit viscometer. The uncertainties are one standard deviation from multiple measurements. The critical temperature of the mixture was $T_c = 48.915$ °C. The background viscosity was taken from Zielesny *et al.* (Ref. 35).

T/°C	η/mPa·s	η/η_B
20.097	2.948±0.024	0.995
24.905	2.556±0.006	1.001
27.620	2.374±0.008	1.005
30.661	2.184±0.008	1.002
34.590	1.974±0.004	0.997
35.483	1.947±0.008	1.004
37.321	1.860±0.008	1.000
38.983	1.807±0.012	1.008
41.182	1.724±0.018	1.007
41.973	1.696±0.012	1.006
43.780	1.643±0.016	1.011
44.235	1.639±0.004	1.018
45.997	1.600±0.004	1.027
48.115	1.587±0.004	1.060
48.245	1.589±0.004	1.064
48.448	1.599±0.004	1.074
48.565	1.607±0.004	1.082
48.699	1.618±0.004	1.092
48.817	1.649±0.004	1.115
48.857	1.660±0.004	1.123
48.885	1.662±0.006	1.125
48.897	1.675±0.006	1.134

TABLE II. Adjustable parameters describing the viscosity of the critical mixture 2-butoxyethanol plus water in the frit viscometer. (The uncertainty in these and other fit parameters is one standard uncertainty, i.e., an estimated standard deviation.)

Adsorption correction	$(Q_0\xi_0)^{x_\eta}$	y	k_d	χ^2
no	0.954 ± 0.005	0.017 ± 0.001	⋯	71
yes	0.873 ± 0.011	0.033 ± 0.002	0.11 ± 0.01	3.6

with $A=2.0961\times10^{-4}$ Pa·s, $B=-214.011$ K, $C=212.434$ K, and where T is the temperature in K. For the adsorption correction we used the correlation length amplitude $\xi_0=0.44$ nm measured by Zielesny *et al.*[35] The direction of the curvature of the liquid–liquid meniscus indicated that water was the component which was preferentially adsorbed onto glass. Therefore, we assumed the viscosity η^{II} of the adsorbed wall layer to be that of pure water.

As shown in Table II, the adsorption correction greatly reduced the systematic deviations of the fit; χ^2 decreased by a factor of 20. Quite reasonably, the fitted value of the adsorption parameter, $k_d=0.11$, indicated that the effective thickness of the adsorption layer was a significant fraction of the correlation length. The adsorption correction also raised the value of the fitted viscosity exponent y from 0.017 to 0.033, thus bringing y much closer toward the values measured by Berg and Moldover (0.042) and by Zielesny *et al.* (0.040).

The remaining discrepancy between y and the expected value 0.04 is likely due to inadequacy of the adsorption correction, which relied on simplified assumptions concerning both the adsorption profile and the capillary geometry. For example, Desai *et al.*[39] found that the strong-field assumption failed to explain their measurements of critical adsorption in a mixture of carbon disulfide and nitromethane. Far from T_c, where adsorption corrections are negligible, the agreement with previous measurements demonstrates the ability of the frit viscometer to measure accurately the viscosity of a noncritical mixture.

2. $N_{2226}B_{2226}$ in diphenyl ether: Background viscosity

Because of the smallness of the viscosity critical exponent, the anomaly is visible in a narrow temperature range of no more than a few K. Thus, although the background viscosity η_B is a function of temperature, in practice this temperature dependence is weak enough that its uncertainty does not greatly affect the fitted value of the exponent y. A common procedure[13,22,40] is to describe the background viscosity by the Arrhenius form

$$\eta_B=A\ \exp\ (B/T), \tag{13}$$

and to fit the measured viscosity by Eq. (1). The background and the critical exponent are thus determined simultaneously. Since the prefactor A becomes lumped with the factor $(Q_0\xi_0)^{x_\eta}$ in Eq. (1), it is not an independent parameter. The temperature coefficient B, however, is an adjustable parameter in addition to the amplitude $A(Q_0\xi_0)^{x_\eta}$ and the exponent y. The data for the frit viscometer, however, are not extensive enough to support the determination of the additional adjustable parameter. Thus, an independent determination of the background viscosity was required for the frit viscometer. Interpolation between a set of off-critical isopleths would have been one option, but the need for filling the viscometer repeatedly with fragile samples made this option impractical. An alternative offered itself because, before studying the new sample in the frit viscometer, we had done a few measurements on a mixture of the same mole fraction but prepared from the batch of spoiled salt from Zhang *et al.*[6] This mixture was found to be far from criticality and in the homogeneous region above 285 K. Below this temperature the mixture separated into phases whose volume ratio was 1:10. The deterioration is not expected to much affect the viscosity of the mixture: At the critical mole fraction, the volume fraction of salt is only 10%, and the viscosity of the decomposed salt has been reported[41] to be only 9%–11% lower than that of the pure salt. The data for the noncritical sample, obtained at three temperatures from 290 to 300 K, sufficed to determine the constants in the Arrhenius equation to be $A=(1.00\pm0.17)\times10^{-6}$ Pa·s and $B=(2597\pm51)$ K. We will show in Sec. V F that the result for B is consistent with the value obtained by fitting to the spiral viscometer's results.

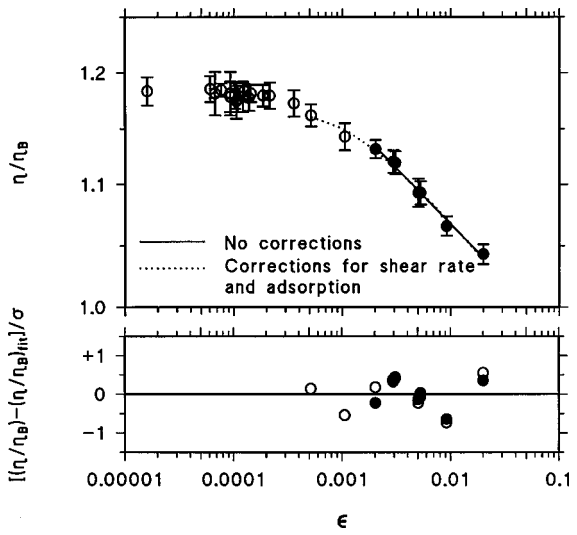

FIG. 6. Viscosity ratio η/η_B of the of the critical mixture $N_{2226}B_{2226}$ in diphenyl ether measured in the frit viscometer. The error bars represent the standard deviation of multiple measurements. The straight line is a fit to data far from T_c without corrections. The dotted line is a fit which includes corrections for both shear rate and adsorption.

3. $N_{2226}B_{2226}$ in diphenyl ether: Critical viscosity

Figure 6 shows the viscosity ratio η/η_B determined for the critical mixture of undegraded $N_{2226}B_{2226}$ in diphenyl ether. Table III contains the results. The background viscosity η_B shown in Fig. 8 is that measured for the noncritical mixture. During the measurement period of 10 days, the critical temperature T_c, which was repeatedly determined by visual observation of phase separation in the reservoir of the viscometer, drifted from 39.351 °C to 39.325 °C. Therefore,

TABLE III. Shear viscosity η of the critical mixture $N_{2226}B_{2226}$ in diphenyl ether measured in the frit viscometer. The uncertainties are one standard deviation from multiple measurements.

T/°C	η/mPa·s	η/η_B
45.597	3.597±0.008	1.042
42.208	4.017±0.008	1.065
40.985	4.255±0.010	1.093
40.907	4.264±0.012	1.093
40.300	4.436±0.010	1.119
40.259	4.446±0.010	1.120
39.969	4.522±0.008	1.131
39.667	4.605±0.012	1.142
39.499	4.700±0.010	1.161
39.450	4.753±0.012	1.172
39.405	4.784±0.012	1.179
39.396	4.787±0.010	1.179
39.383	4.799±0.008	1.181
39.381	4.780±0.012	1.177
39.377	4.807±0.007	1.183
39.376	4.787±0.014	1.178
39.372	4.781±0.012	1.176
39.371	4.771±0.016	1.174
39.370	4.793±0.012	1.179
39.367	4.787±0.014	1.178
39.367	4.799±0.020	1.181
39.362	4.812±0.006	1.184
39.359	4.799±0.020	1.181
39.357	4.816±0.012	1.185
39.343	4.811±0.013	1.183

at each temperature, the reduced temperature was calculated from the value of T_c interpolated to the time of the viscosity measurement.

Figure 6 clearly shows a viscosity anomaly. In the restricted range of reduced temperatures from $0.002<\epsilon<0.02$ we could describe the data by the simple power law fit of Eq. (1) with a critical exponent $y=0.037\pm0.004$, where 0.004 is one standard uncertainty from the fit. This value of y is consistent with that for an Ising fluid. The deviation of the data from a simple power law at reduced temperatures below 0.002 is due to both adsorption and shear rate effects. As shown in Table IV, when the corrections for both adsorption and shear rate were included, the lower bound of the range of fitted data could be decreased by a factor of 4 without large systematic deviations.

V. SPIRAL VISCOMETER

A. Description

Because both shear and adsorption affect the performance of the frit viscometer, we decided to substantially reduce these effects by a redesign of the impedance in the form of a very long capillary. The capillary's inner diameter of 203 ± 10 μm was large enough to eliminate the need for adsorption corrections. (The uncertainty is the manufacturer's stated tolerance). By choosing a very small difference between the meniscus heights of the right and left arms, the pressure head, and thus the shear rate, could be made very small.

A sketch of the spiral viscometer is shown in Fig. 2. The spiral shape of the 1.1 m long capillary made it possible to fit the viscometer into a temperature-controlled water bath of modest size. Only a small portion of the sample, contained entirely within the capillary, was used for a viscosity measurement. This portion formed a spiral column bounded by two menisci, one in the left vertical arm of the capillary and the other in the right vertical arm. This symmetry caused cancellation of the considerable pressures due to surface tension at the ends of the liquid column. The horizontal distance between the two vertical straight arms of the capillary, 0.15 m, was made large enough so that when the viscometer was tilted, surface tension would not prevent drainage of liquid from the capillary. The two larger side arms had the same purpose as the cold finger in the frit viscometer, and they allowed the liquid sample to mix at a temperature well above T_c before a small portion of it was loaded into the capillary. The capillary protruded into the viscometer's interior to prevent drainage of any liquid condensing above the capillary's entrance during the viscosity measurement. Had the inlet been shaped as a funnel, even a small amount of drainage would have created a droplet clogging the capillary at the top.

B. Cleaning and filling

The cleaning procedure for the spiral viscometer was similar to that for the frit viscometer. However, the spiral viscometer was dried under vacuum at 90 °C.

Unlike the frit viscometer, the spiral viscometer was extremely susceptible to clogging by a single dust particle. Vacuum drying minimized the viscometer's exposure to dust, and no dust particle was seen in the viscometer during the viscosity measurements. Absence of dust was indicated also by the viscosity measurements themselves. The meniscus fell with an exponential time dependence which was reproducible.

C. Operation

The temperature control, the determination of T_c, and the flushing procedures were similar to those used for the frit viscometer. Repeatedly during the experiment, the value of T_c was determined by visual observation of phase separation in the reservoir of the viscometer. By tilting the viscometer

TABLE IV. Fit parameters for the viscosity of the critical mixture $N_{2226}B_{2226}$ in diphenyl ether measured in the frit viscometer.

Range of ϵ	Adsorption	Shear rate	$(Q_0\xi_0)^{x_\eta}$	y	k_d	χ^2
$0.002<\epsilon<0.02$	no	no	0.90±0.01	0.037±0.004	···	3.5
$0.0005<\epsilon<0.02$	no	yes	0.93±0.005	0.031±0.001	···	84
$0.0005<\epsilon<0.02$	yes	yes	0.88±0.011	0.044±0.003	0.32±0.03	20

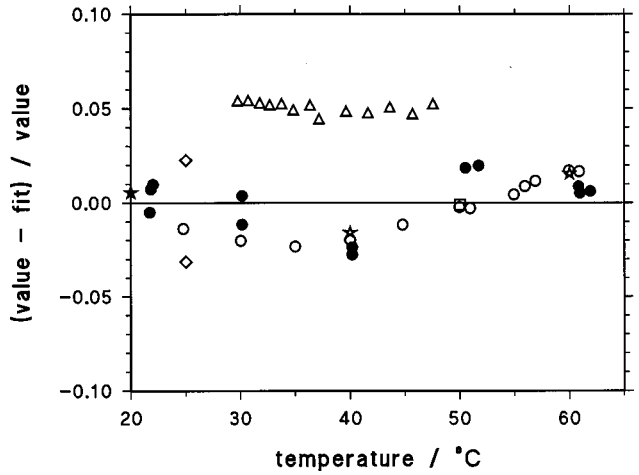

FIG. 7. Deviations of measurements of the viscosity of diphenyl ether from the fit describing the data obtained in the spiral viscometer. The closed circles (○) are from the spiral viscometer, the open circles (○) are from measurements made in a conventional capillary viscometer, and the remainder are various literature data: Dreisbach (★) (Ref. 45), Landolt-Börnstein (◇) (Refs. 46 and 47), Lide (□) (Ref. 48), Dodd and Hu (△) (Ref. 44).

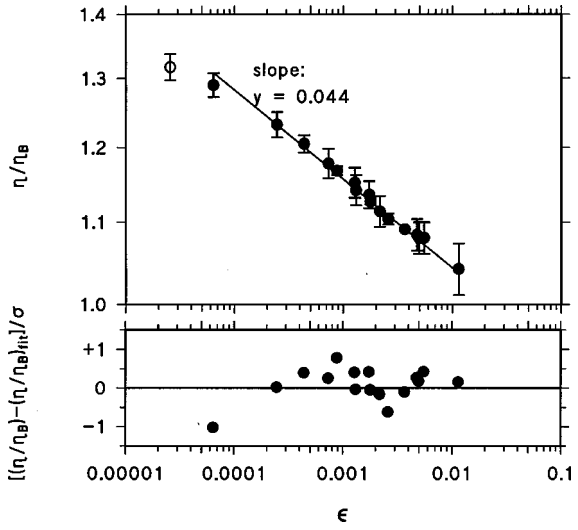

FIG. 9. Viscosity ratio η/η_B of the of the critical mixture $N_{2226}B_{2226}$ in diphenyl ether measured in the spiral viscometer. The point closest to T_c was excluded due to the 5 mK irreproducibility in T_c. The error bars represent the standard deviation of multiple measurements. Above $\epsilon=0.0005$, shear rate effects were less than 0.5% and adsorption effects were negligible. The straight line is a fit made without corrections for shear rate or adsorption.

we filled the capillary with the thoroughly mixed sample, taking care to avoid vapor bubbles. During a viscosity measurement, the only fluid measured was that of the liquid column contained within the capillary's very small volume of $0.03\ \mathrm{cm}^3$. The column's length was such that the liquid–vapor meniscus was located in the upper half of both vertical capillary arms. By measuring the equilibrium positions of the two menisci relative to the ends of the capillary we obtained the length l of the column for each viscosity measurement. This accounted for changes in l caused by, for example, thermal expansion of the sample.

A viscosity measurement was begun by tilting the viscometer to displace the liquid column from its equilibrium position. After returning the viscometer to an upright position, the meniscus in one arm rose and that in the other arm fell. We periodically recorded the position of the meniscus in each arm and then fit the exponential fall time τ. The falling meniscus left behind a drainage film[42] on the walls of the capillary. This depletion of the liquid column decreased the time constant of the falling meniscus by a few percent, especially at high viscosities. Therefore, we used only the data for the rising meniscus.

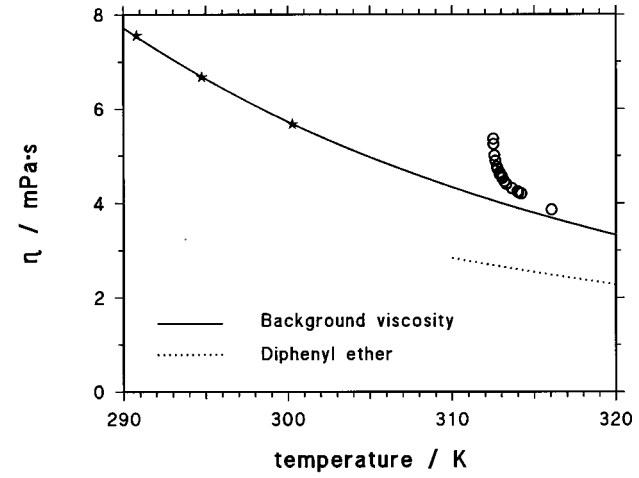

FIG. 8. The viscosity of pure diphenyl ether and the viscosity of the critical mixture $N_{2226}B_{2226}$ in diphenyl ether measured in the spiral viscometer. Also shown is the viscosity of the noncritical mixture (★) measured in the frit viscometer. The solid line represents the extrapolation of these data to higher temperatures.

D. Model of the viscometer

The model of the spiral viscometer was similar to that of the frit viscometer in that the observed height of the meniscus was fit by an exponential in time. However, because the measured fluid was contained entirely in the flow impedance, the viscosity η was derived from the exponential fall time τ according to

$$\eta=\frac{\rho g R^2 \tau}{4l}. \tag{14}$$

As with conventional capillary viscometers, the viscosity uncertainty is dominated by the uncertainty in the capillary radius R. However, the viscosity determination is proportional to R^2, not R^4 as is the case for conventional viscometers. Thus, before calibration, the 5% uncertainty in R caused only an 11% uncertainty in the viscosity.

The radius of the capillary was the same in both vertical arms. If the two radii had differed, surface tension would have caused a difference between the left and right equilibrium meniscus heights. The two heights agreed to better than $\Delta h=0.5$ mm, implying that the left and right radii were consistent to within

$$\frac{\Delta R}{R}=\frac{\rho g R \Delta h}{2\sigma}\simeq 0.01. \tag{15}$$

TABLE V. Values of the viscosity exponent obtained from fits to the viscosity measured in the spiral viscometer. The first row contains the fit based on nominal values, and the other rows describe the fits obtained upon varying the background viscosity, the critical temperature, and the fitting range's minimum reduced temperature.

Background	Minimum ϵ	T_c/K	B/K	y	χ^2
		background free or fixed			
free	6.4×10^{-5}	312.490	2943±798	0.043±0.005	2.7
fixed	6.4×10^{-5}	312.490	2597	0.044±0.002	2.8
		T_c varied			
fixed	6.4×10^{-5}	312.485	2597	0.046±0.002	2.0
fixed	6.4×10^{-5}	312.495	2597	0.043±0.002	5.0
		minimum ϵ varied			
fixed	2.6×10^{-5}	312.490	2597	0.043±0.002	6.8
fixed	2.5×10^{-4}	312.490	2597	0.046±0.002	1.5

(The surface tension, $\sigma\approx0.03$ N·m^{-1}, was estimated as that of a typical organic liquid.) A height-dependent radius would also have caused the measured viscosity to depend on flow direction. No such dependence was seen.

Corrections for the kinetic energy of the fluid were negligible, as indicated by the small value of the dimensionless parameter $l/(g\tau^2)$. Corrections due to the curvature of the capillary were also negligible.

Near T_c, the time constant τ which characterized the meniscus movement was ~180 s. The typical shear rate for the critical ionic mixture was thus

$$S=\frac{4\rho gRh}{15\eta l}=\frac{16}{15}\frac{h}{R\tau}\simeq1.2\ \ \mathrm{s}^{-1}, \tag{16}$$

where $h=2$ cm was the typical initial difference between the heights of the left and right meniscus.

E. Calibration

We checked the model of the viscometer by measuring the viscosity of pure diphenyl ether at five temperatures in the range from 20 to 60 °C. To convert the observed time constants into viscosities, we used the density of diphenyl ether measured by Kleemeier[43]

$$\rho=(1091.8\ \mathrm{kg\cdot m^{-3}})[1-(7.55\times10^{-4})(T-T_0)], \tag{17}$$

where $T_0=273.15$ K, and T is the temperature in Kelvin. The viscosity data were then fit by a two-parameter Arrhenius temperature function. Figure 7 compares the values obtained in the spiral viscometer with values obtained in a conventional capillary viscometer and with values obtained by others. In the range from 20 °C to 60 °C, where the viscosity varied from 1.8 to 4.0 mPa·s, the values from the spiral viscometer and the conventional viscometer agreed to within 2%. Over the range of temperatures from 30 °C to 50 °C, the values from the spiral viscometer disagreed with those of Dodd and Mi[44] by as much as 8%. Dodd and Mi did not state the accuracy or the units of their viscosity data. The agreement with the other literature values[45–48] was within 3%. Based on these comparisons, we estimate that viscosities calculated with the spiral viscometer's nominal radius of $R=203$ μm had an uncertainty of 3%.

TABLE VI. The amplitude $(Q_0\xi_0)^{x_\eta}$ derived from viscosity measurements.

Fluid	ξ_0/nm	$(Q_0\xi_0)^{x_\eta}$	y	Reference
pure fluids				
CO_2	0.15	0.76	0.041	Ref. 40
Xe	0.19	0.78	0.041	Ref. 40
nonionic mixtures				
n-hexane+nitrobenzene	0.354	0.88	0.043	Ref. 54
2-butoxyethanol+water	0.44	0.84	0.040	Ref. 35
ionic mixtures				
N_{4444} picrate+C_{13}OH	0.31	0.85	0.043	Ref. 21
ethylammonium nitrate+C_8OH	0.3	0.89	0.031	Ref. 24
$N_{2226}B_{2226}$+diphenyl ether	1.4	0.86±0.01	0.044	(This work)

F. Results: Critical $N_{2226}B_{2226}$ in diphenyl ether

Figure 8 shows the viscosity determined for the critical mixture of $N_{2226}B_{2226}$ in diphenyl ether. Also shown are the fits to the viscosity of diphenyl ether and to the noncritical mixture. Figure 9 shows the viscosity ratio η/η_B, where the background viscosity was equated with the fit to the values obtained for the noncritical mixture in the frit viscometer. The critical temperature, $T_c=(312.49\pm0.01)$ K, where the

TABLE VII. Shear viscosity η of the critical mixture $N_{2226}B_{2226}$ in diphenyl ether measured in the spiral viscometer. The uncertainties are one standard deviation from multiple measurements. The critical temperature of the mixture was $T_c=39.34$ °C.

T/°C	η/mPa·s	η/η_B
42.900	3.859±0.031	1.042
41.060	4.195±0.020	1.080
40.890	4.216±0.020	1.080
40.825	4.239±0.020	1.084
40.489	4.305±0.001	1.091
40.150	4.394±0.007	1.104
40.018	4.450±0.020	1.114
39.896	4.517±0.004	1.127
39.882	4.553±0.018	1.136
39.750	4.593±0.020	1.142
39.740	4.637±0.020	1.152
39.615	4.714±0.006	1.168
39.569	4.764±0.020	1.178
39.477	4.884±0.012	1.205
39.417	5.001±0.018	1.232
39.360	5.243±0.018	1.290
39.348	5.356±0.020	1.317

uncertainty is one standard deviation from the mean of multiple measurements, was defined as the temperature at which demixing occurred in the reservoir arms. As with the frit viscometer, demixing was indicated by Schlieren effects.

We fit the data (Table VII) with the simple power law of Eq. (1), where the background viscosity η_B was represented by the Arrhenius form of Eq. (13). The point closest to T_c was not included in the fit due to the 5 mK irreproducibility in T_c. The fitting parameters were the product $A(Q_0\xi_0)^{x_\eta}$, the background parameter B, and the viscosity exponent y. The fitted value of the exponent is $y=0.043\pm0.005$, where the uncertainty is one standard deviation from the fit. This value is within the range $0.0404<y<0.0444$ measured in four nonionic mixtures by Berg and Moldover. Also, the range defined by B and its uncertainty includes the value of $B=2597\pm51$ K obtained from the noncritical sample.

We checked the sensitivity of the value of the viscosity exponent to various changes in the fitting procedure (Table V). We fixed the background at the values determined from the noncritical sample. We decreased and increased the value of T_c by its uncertainty of 5 mK. We also modified the range of the fit by removing or adding points close to T_c. In all cases the critical exponent stayed within the limits of the original value from the three-parameter fit and its uncertainty. For the case of fixed background, the value of the nonuniversal critical amplitude was $(Q_0\xi_0)^{x_\eta}=0.86\pm0.01$. This value is in the same range as found for other binary mixtures, both ionic and nonionic, and it is $\sim10\%$ higher than that for pure fluids (Table VI).

VI. CONCLUSION

Until recently, the ionic mixture $N_{2226}B_{2226}$ in diphenyl ether was the leading candidate for a mean-field fluid composed of small molecules. Measurements of the coexistence curve[4,5] and the turbidity[6] had indicated mean-field static behavior. In contrast, the present measurements show a critical viscosity enhancement similar to that seen in Ising fluids. Such an enhancement is not expected in either a mean-field fluid[15] or a fluid with sufficiently long-ranged forces.[14]

The Ising character indicated by the viscosity measurements is also indicated by other recent measurements. Turbidity measurements made on the same sample[7] indicated a better consistency with Ising-type behavior ($\gamma=1.24$) than with mean-field behavior. The cause of the disagreement with the earlier turbidity measurements[6] is unclear. However, careful examination of the data from the earlier measurements revealed a time dependence not seen in the present sample. Coexistence curve measurements made on a sample prepared from the same batch of $N_{2226}B_{2226}$ salt also found Ising-type behavior.[43]

To study the viscosity of the present ionic binary mixture we developed two novel viscometers. The frit viscometer, which also had low shear rates, exhibited a large adsorption effect which reduced the apparent viscosity near the critical point. Replacement of the frit by an impedance with a well-characterized geometry, such as an array of parallel capillaries, would enable a direct investigation of this interesting phenomenon. The spiral viscometer described here may be useful for other applications where very low shear rates are required.

ACKNOWLEDGMENTS

We thank Dean Ripple for helpful discussion on experimental problems such as drainage and adsorption. Jack Douglas was a constant source of encouragement and ideas, including the use of viscosity to discern mean-field versus Ising critical behavior, and he carefully read the manuscript. We acknowledge useful communications with Reinhard Folk, Richard Ferrell, and George Stell concerning dynamic critical exponents in fluids with long-range forces. We thank Jeff Anderson for his patient skill in constructing the viscometers. We acknowledge Cornelia Rybarsch-Steinke's measurements of the viscosity of diphenyl ether. We thank Malte Kleemeier for providing his data on the density of diphenyl ether. Arno Laesecke alerted us to the possibility of electrokinetic effects. One of us (S.W.) acknowledges a grant from the Alexander von Humboldt Stiftung permitting her to carry out this work at NIST.

APPENDIX A: ADSORPTION CORRECTIONS

We had no detailed knowledge of either the geometry of the frit's pores or of the adsorption scaling function $P(z/\xi)$. Therefore, the following correction was devised. The velocity profile was assumed to be similar to Poiseuille flow within a circular tube, except that the viscosity was a function of the radius r within the tube (see Fig. 3). This function had only two values, namely

$$\eta=\eta^I \quad \text{in the bulk, for } 0<r<(R-d), \tag{A1}$$

$$\eta=\eta^{II} \quad \text{near the wall, for } (R-d)<r<R. \tag{A2}$$

In the tube's interior the viscosity was the usual ''bulk'' viscosity η^I characteristic of the critical composition, and near the wall the viscosity η^{II} was that of a fluid whose composition was shifted due to preferential adsorption by the glass wall. We modeled the scaling function $P[(R-r)/\xi]$ by a layer of thickness d. The layer was assumed to be proportional to the correlation length, namely $d\equiv k_d\xi$, where k_d was a constant independent of temperature. The velocity profiles for the bulk center region $u^I(r)$ and the wall region $u^{II}(r)$ were thus

$$u^I(r)=\frac{r^2\Delta p}{4l\eta^I}+c_2^I,$$

$$u^{II}(r)=\frac{r^2\Delta p}{4l\eta^{II}}+c_2^I+c_1^{II}\ln r. \tag{A3}$$

The constants c_1^{II}, c_2^I, and c_2^{II} were determined by the requirements that the velocity and its radial derivative are continuous at $r=R-d$ and that the velocity at the wall is zero

$$u^I(R-d)=u^{II}(R-d),$$

$$\eta^I\left(\frac{\partial u^I}{\partial r}\right)_{R-d}=\eta^{II}\left(\frac{\partial u^{II}}{\partial r}\right)_{R-d}, \tag{A4}$$

$$u^{II}(R)=0.$$

We thus obtained the volume flow per unit time.

$$\dot{V}=\frac{\pi R^4\Delta p}{8l\eta^I}\left\{1+\left[\frac{\eta^I-\eta^{II}}{\eta^{II}}\right]\left[4\left(\frac{d}{R}\right)-6\left(\frac{d}{R}\right)^2+4\left(\frac{d}{R}\right)^3-\left(\frac{d}{R}\right)^4\right]\right\}. \tag{A5}$$

Instead of measuring the bulk viscosity η^I, we measured the effective viscosity η, defined by

$$\eta=\eta^I\left\{1+\left[\frac{\eta^I-\eta^{II}}{\eta^{II}}\right]\left[-4\left(\frac{k_d\xi}{R}\right)+6\left(\frac{k_d\xi}{R}\right)^2-O\left(\frac{k_d\xi}{R}\right)^3\right]\right\}. \tag{A6}$$

Note that the difference between η and η^I disappears when either the layer's thickness $k_d\xi$ or the viscosity contrast $(\eta^I-\eta^{II})$ goes to zero.

Our model is in the spirit of a model for the flow of liquids through a porous medium, which is given in the last part of the paper by Debye and Cleland.[49] These authors assumed a constant velocity in the boundary layer. The velocity at the wall being finite, a friction force is generated between the boundary layer and the wall. In our application, the model would require adjustment of two parameters, the friction force and the layer thickness, whereas in our model only one parameter needs adjustment. Introducing yet another adjustable parameter, however, is clearly not warranted, given the uncertainty of our data.

APPENDIX B: SHEAR CORRECTION

Following Oxtoby,[50] the shear-dependent viscosity $\eta(S)$ of a mixture of critical composition is

$$\eta(S)=\eta(0)[1-\Delta(\lambda)], \tag{B1}$$

where $\eta(0)$ is the viscosity in the limit of zero shear rate. The correction function,

$$\Delta(\lambda)=\begin{cases}0.0214+0.011\,55(\ln\lambda)+0.001\,47(\ln\lambda)^2 & \text{for } 0.1<\lambda<10\\ \frac{1}{3}x_\eta\ln(\lambda/0.45) & \text{for } 10<\lambda\end{cases}, \tag{B2}$$

depends on the dimensionless parameter

$$\lambda\equiv(\eta\xi^3S)/(k_BT). \tag{B3}$$

We used Eq. (B2) to adjust the observed apparent viscosity values to their zero-shear values. A typical shear rate for the critical mixture $N_{2226}B_{2226}$ was estimated to be $S\approx 40\ s^{-1}$. By eliminating points close to the critical temperature, shear corrections in the frit viscometer were always kept below 0.5%.

APPENDIX C: ELECTROKINETIC EFFECTS

Most solid surfaces are charged and carry a surface potential $\Psi=\Psi_0$. When an ionic fluid is in contact with the wall of a capillary, a diffusive electrical double layer forms. If the fluid flows, an additional electric body force results that affects the flow and increases the viscosity. Rice and Whitehead[51] calculated the increase of the viscosity for capillary flow. The charge distribution in the double layer was calculated by solving the Poisson–Boltzmann equation in the Debye–Hückel linear approximation, which implies $\varepsilon\Psi<k_BT$, where ε is the dielectric constant. The relevant dimensionless parameter is κR with κ the Debye–Hückel inverse length and R the radius of the capillary. The authors found that the viscosity may be increased by up to a factor of 6 in the range of κR between 0 and 10, for the modest surface potentials, Ψ_0 up to 50 mV, for which the Debye–Hückel theory is valid.

Mean-field calculations in the framework of the restricted primitive model (RPM)[52,53] show that 30%–50% of the salt is dissociated at the critical point. Using this dissociation rate, we have estimated the value of κ to be $6\times10^9\ m^{-1}$. Since the capillary radius of the frit viscometer is $\sim3\times10^{-6}$ m, the dimensionless product κR is of the order 1.8×10^4, far exceeding the range in which electrokinetic effects are important.

[1] J. M. H. Levelt Sengers and J. Given, Mol. Phys. **80**, 899 (1993).
[2] J. M. H. Levelt Sengers, A. Harvey, and S. Wiegand, in *Equations of State for Fluids and Mixtures*, edited by R. F. Kayser, J. V. Sengers, M. B. Ewing, and C. Peters (Blackwell Scientific, Oxford, 1998), in press.
[3] K. Pitzer, J. Phys. Chem. **99**, 13070 (1995).
[4] R. Singh and K. Pitzer, J. Am. Chem. Soc. **110**, 8723 (1988).
[5] R. Singh and K. Pitzer, J. Chem. Phys. **92**, 6775 (1990).
[6] K. Zhang, M. Briggs, R. Gammon, and J. L. Sengers, J. Chem. Phys. **97**, 8692 (1992).
[7] S. Wiegand, J. M. H. Levelt Sengers, K. J. Zhang, M. E. Briggs, and R. W. Gammon, J. Chem. Phys. **106**, 2777 (1997).
[8] P. Hohenberg and B. Halperin, Rev. Mod. Phys. **49**, 435 (1977).
[9] T. Ohta, J. Phys. Chem. **10**, 791 (1977).
[10] J. Sengers, Int. J. Thermophys. **6**, 203 (1985).
[11] J. Bhattacharjee, R. Ferrell, R. Basu, and J. Sengers, Phys. Rev. A **24**, 1469 (1981).
[12] H. Hao, R. Ferrell, and J. Bhattacharjee, 1997 preprint; H. Hao, Doctoral thesis, University of Maryland, 1991.
[13] R. Berg and M. Moldover, J. Chem. Phys. **89**, 3694 (1988).
[14] R. Folk and G. Moser, Phys. Rev. E **49**, 3128 (1994).
[15] J. Douglas, Macromolecules **25**, 1468 (1992).
[16] R. Mountain and R. Zwanzig, J. Chem. Phys. **48**, 1451 (1968).
[17] A. C. Flewelling, R. J. DeFonseka, N. Khaleeli, J. Partee, and D. T. Jacobs, J. Chem. Phys. **104**, 8048 (1996).
[18] C. Bagnuls and C. Bervillier, Phys. Lett. A **107**, 299 (1985).
[19] C. Bagnuls and C. Bervillier, Phys. Lett. A **112**, 477 (1985).
[20] C. Bervillier and C. Godreche, Phys. Rev. B **21**, 5427 (1980).
[21] M. Kleemeier, S. Wiegand, T. Derr, V. Weiss, W. Schröer, and H. Weingärtner, Ber. Bunsenges. Phys. Chem. **100**, 27 (1996).
[22] J. Nieuwoudt and J. Sengers, J. Chem. Phys. **90**, 457 (1989).
[23] T. Narayanan and K. Pitzer, J. Chem. Phys. **102**, 8118 (1995).
[24] A. Oleinikova and M. Bonetti, J. Chem. Phys. **104**, 3111 (1996).

[25] W. Schröer, S. Wiegand, and H. Weingärtner, Ber. Bunsenges. Phys. Chem. **97**, 975 (1993).
[26] D. Beysens, A. Bourgou, and G. Paladin, Phys. Rev. A **30**, 2686 (1984).
[27] W. Ford, R. Hauri, and D. Hart, J. Org. Chem. **38**, 3916 (1973).
[28] N. Weiden, B. Wittekopf, and K. Weil, Ber. Bunsenges. Phys. Chem. **94**, 353 (1990).
[29] R. Singh (private communication).
[30] K. Zhang (private communication).
[31] M. Fisher and P. de Gennes, C. R. Acad. Sci. Ser. B **287**, 207 (1978).
[32] In order to describe materials and experimental procedures adequately, it is occasionally necessary to identify commercial products by manufacturers' name or label. In no instance does such identification imply endorsement by the National Institute of Standards and Technology, nor does it imply that the particular product or equipment is necessarily the best available for the purpose.
[33] R. Bird, W. Stewart, and E. Lightfoot, *Transport Phenomena* (Wiley, New York, 1960), Chap. 2.
[34] F. Goncalves, J. Kestin, and J. Sengers, Int. J. Thermophys. **12**, 1013 (1991).
[35] A. Zielesny, J. Schmitz, S. Limberg, A. G. Aizpiri, S. Fusenig, and D. Woermann, Int. J. Thermophys. **15**, 67 (1994).
[36] K. Hamano, T. Kawazura, T. Koyama, and N. Kuwahara, J. Chem. Phys. **82**, 2718 (1985).
[37] C. Baaken, L. Belkoura, S. Fusenig, Th. Muller-Kirschbaum, and D. Woermann, Ber. Bunsenges. Phys. Chem. **94**, 150 (1990).
[38] J. Schmitz, L. Belkoura, and D. Woermann, J. Chem. Phys. **101**, 476 (1994).
[39] N. Desai, S. Peach, and C. Franck, Phys. Rev. E **52**, 4129 (1995).
[40] R. Berg and M. Moldover, J. Chem. Phys. **93**, 1926 (1990).
[41] W. Ford and D. Hart, J. Phys. Chem. **80**, 1002 (1976).
[42] L. Landau and B. Levich, Acta Physicochim. URSS **17**, 42 (1942).
[43] M. Kleemeier (private communication).
[44] C. Dodd and H. P. Mi, Proc. Phys. Soc. London, Sect. B **62**, 454 (1949).
[45] R. Dreisbach, *Physical Properties of Chemical Substances* (Dow Chemical Company, Midland Michigan, 1954), pp. 10-3.
[46] Landolt-Börnstein, *Hauptwerk 1* (Springer-Verlag, Berlin, 1923).
[47] Landolt-Börnstein, *Ergänzungsband 1* (Springer-Verlag, Berlin, 1927).
[48] D. Lide, *Handbook of Organic Solvents* (CRC, Boca Raton, Florida, 1995), p. 198.
[49] P. Debye and R. Cleland, J. Appl. Phys. **30**, 843 (1959).
[50] D. Oxtoby, J. Chem. Phys. **62**, 1463 (1975).
[51] C. Rice and R. Whitehead, J. Chem. Phys. **69**, 4017 (1965).
[52] Y. Levin and M. Fisher, Physica A **225**, 164 (1996).
[53] V. Weiss and W. Schröer, J. Chem. Phys. **106**, 1930 (1997).
[54] J. Rouch, P. Tartaglia, and S. Chen, Phys. Rev. A **37**, 3046 (1988).